Production of High Melting Resistance Ice via CO_2 Utilization

Taweechok Sochiphan

A Report Submitted in Partial Fulfillment of the Requirements
for the Degree of Bachelor of Engineering (Petrochemical Engineering)
Department of Chemical Engineering, School of Engineering,
King Mongkut's Institute of Technology Ladkrabang
Academic Year 2020

การผลิตน้ำแข็งละลายช้าโดยการใช้ประโยชน์จากคาร์บอนไดออกไซด์

ทวีโชค โศจิพันธุ์

ปริญญานิพนธ์นี้เป็นส่วนหนึ่งของการศึกษาตามหลักสูตร

วิศวกรรมศาสตรบัณฑิต สาขาวิชาวิศวกรรมปิโตรเคมี

ภาควิชาวิศวกรรมเคมี คณะวิศวกรรมศาสตร์

สถาบันเทคโนโลยีพระจอมเกล้าเจ้าคุณทหารลาดกระบัง

ปีการศึกษา 2563

Title	Production of High Melting Resistance Ice via CO_2 Utilization
By	Mr. Taweechok Sochiphan
Field of Study	Petrochemical Engineering
Advisor	Asst.Prof.Dr. Surat Areerat

Accepted by the School of Engineering, King Mongkut's Institute of Technology Ladkrabang in Partial Fulfillment of the Requirements for the Degree of Bachelor of Engineering (Petrochemical Engineering).

Thesis Committee

S. Areerat ________________________ Chairman

(Asst.Prof.Dr. Surat Areerat)

Anchaleeporn W. Lothongkum ________________________ Committee

(Assoc. Prof. Dr. Anchaleeporn Waritswat Lothongkum)

Tanawan Pinnarat. ________________________ Committee

(Asst.Prof.Dr. Tanawan Pinnarat)

Title Production of High Melting Resistance Ice via CO_2 Utilization
By Mr. Taweechok Sochiphan
Advisor Asst.Prof.Dr. Surat Areerat
Field of Study Petrochemical Engineering
Affiliation Department of Chemical Engineering, School of Engineering, King Mongkut’s Institute of Technology Ladkrabang

Abstract

In this work, carbon dioxide (CO_2) was utilized to produce high melting resistance ice. The prototype equipment consisted of two main components: a vacuum degassing unit and a water-pre-cooling unit, both of which aimed to improve the quality of water used to produce ice. To begin with, water was degassed using a vacuum unit. This was accomplished by feeding carbon dioxide gas as a working fluid through a venturi nozzle, which generated a venturi jet effect above the vacuum chamber. Then, the degassed water was chilled in a double-pipe heat exchanger using liquid carbon dioxide. The heat exchanger's unique design has an inner copper tube drive system that converts the liquid carbon dioxide to vapor which flows directly into the venturi nozzle for degassing in the vacuum chamber. The effects of various carbon dioxide supply conditions, including temperature and pressure, on the venturi nozzle and the double-pipe heat exchanger, were analyzed in terms of vacuum stage level and degassed water temperature at the outlet position. Further, the prototype equipment operated continuously to make water to produce ice with a high melting resistance by analyzing its melting rate. This rate was reduced from 2.8×10^{-3} g/s for normal reverse osmosis water to 2.4×10^{-3} g/s for treated water at a given degassing pressure of 90.2 kPa and a pre-cooling temperature of 9 °C. The results indicated that the treatments enhance the melting resistance of ice.

Keywords: Carbon dioxide utilization, Venturi nozzle, Vacuum degassing, Ice

เรื่อง	การผลิตน้ำแข็งละลายช้าโดยการใช้ประโยชน์จากคาร์บอนไดออกไซด์
โดย	นายทวีโชค โศจิพันธุ์
อาจารย์ที่ปรึกษา	ผศ.ดร.สุรัตน์ อารีรัตน์
สาขาวิชา	วิศวกรรมปิโตรเคมี
สังกัด	ภาควิชาวิศวกรรมเคมี คณะวิศวกรรมศาสตร์
	สถาบันเทคโนโลยีพระจอมเกล้าเจ้าคุณทหารลาดกระบัง

บทคัดย่อ

งานนี้ศึกษาการใช้ประโยชน์ของคาร์บอนไดออกไซด์เพื่อผลิตน้ำแข็งที่ละลายช้า โดยอุปกรณ์ต้นแบบประกอบด้วยสองส่วนหลัก: หน่วยกำจัดแก๊สแบบสุญญากาศและหน่วยทำความเย็นสำหรับน้ำที่ใช้ผลิต ซึ่งทั้งสองส่วนมีวัตถุประสงค์เพื่อปรับปรุงคุณภาพของน้ำที่ใช้ผลิตน้ำแข็ง ในขั้นต้นน้ำถูกกำจัดแก๊สหรือกำจัดอากาศโดยระบบสุญญากาศ ซึ่งทำได้โดยการใช้แก๊สคาร์บอนไดออกไซด์ป้อนผ่านหัวฉีดเวนทูรีเพื่อสร้างสภาวะสุญญากาศในระบบที่น้ำไหลผ่าน หลังจากนั้นน้ำที่ผ่านการกำจัดแก๊สจะถูกทำให้เย็นด้วยคาร์บอนไดออกไซด์เหลวในเครื่องแลกเปลี่ยนความร้อนแบบท่อสองชั้น เครื่องแลกเปลี่ยนความร้อนที่ออกแบบมาเฉพาะนี้ ประกอบด้วยท่อทองแดงด้านในที่ป้อนคาร์บอนไดออกไซด์ในสถานะของเหลวไหลผ่านเพื่อทำให้ระเหยกลายเป็นไอและไหลไปยังหัวฉีดเวนทูรีสำหรับขั้นตอนการกำจัดแก๊สต่อไป ผลกระทบของสภาวะการจ่ายคาร์บอนไดออกไซด์ ที่แตกต่างกันในแง่ของอุณหภูมิและความดัน ถูกนำมาใช้วิเคราะห์ผลกระทบต่อหัวฉีดเวนทูรีและเครื่องแลกเปลี่ยนความร้อนแบบท่อสองชั้นในแง่ของระดับขั้นสุญญากาศและอุณหภูมิของน้ำที่เย็นลงที่ตำแหน่งทางออก นอกจากนี้อุปกรณ์ต้นแบบยังทำงานได้อย่างต่อเนื่องเพื่อผลิตน้ำแข็งที่ละลายช้า โดยวิเคราะห์จากอัตราการหลอมเหลวของน้ำแข็ง จากการศึกษาพบว่าอัตราการหลอมเหลวของน้ำแข็งลดลงจาก 2.8×10^{-3} g/s สำหรับน้ำรีเวอร์สออสโมซิสปกติเป็น 2.4×10^{-3} g/s สำหรับน้ำที่ผ่านการปรับปรุงคุณภาพแล้วที่ความดันในการกำจัดแก๊ส 90.2 kPa สำหรับขั้นตอนการกำจัดแก๊สและ 9 °C สำหรับขั้นตอนการทำความเย็น ผลการศึกษาพบว่าเครื่องต้นแบบมีความสามารถในการเพิ่มความต้านทานการละลายของน้ำแข็ง

คำสำคัญ: การใช้ประโยชน์จากคาร์บอนไดออกไซด์ หัวฉีดเวนทูรี ระบบกำจัดแก๊สสุญญากาศ น้ำแข็ง

Acknowledgment

I would like to express my sincere thanks to my advisor, Asst. Prof. Dr. Surat Areerat, for his suggestions, support and providing the necessary materials and workspace for my research. Moreover, I would like to express my gratitude to the committee members, Assoc. Prof. Dr. Anchaleeporn Waritswat Lothongkum and Asst. Prof. Dr. Tanawan Pinnarat, for their recommendations and comments.

I would also like to thank all the professors in the Department of Chemical Engineering, King Mongkut's Institute of Technology Ladkrabang, and the authorities, Mr. Pisan Ponpo and Dr. Eakarach Bumrungthaichaichan.

Lastly, I would really like to express my appreciation to my family for their encouragement and support.

Taweechok Sochiphan

Table of Contents

Table of Contents (Cont.)

Table of Contents (Cont.)

List of Figures

List of Tables

NOMENCLATURE

x_i	Mole fraction of specie i in liquid phase
H_i	Henry's constant, bars
x_i	Mole fraction of specie i in vapor phase
P_A	Ambient pressure, bars
Ma	Mach number
v	Fluid flow velocity, m/s
c	Speed of sound, m/s
T_{CO_2}	Local temperature of carbon dioxide, K
$T_{CO_2,0}$	Inlet temperature of carbon dioxide, K
P_{CO_2}	Local pressure of carbon dioxide, bars
$P_{CO_2,0}$	Inlet pressure of carbon dioxide, bars
A	Local cross-sectional area, m^2
A^*	Cross-sectional area at throat, m^2
k	Heat capacity ratio
$P_{H_2O,I}$	Inlet pressure of water, kPa
$v_{H_2O,I}$	Inlet velocity of water, m/s
$h_{H_2O,I}$	Inlet height of water from reference point, m
$P_{H_2O,O}$	Outlet pressure of water, kPa
$v_{H_2O,O}$	Outlet velocity of water, m/s
$h_{H_2O,O}$	Outlet height of water from reference point, m
ρ_{H_2O}	Density of water, kg/m^3

g Gravitational constant, m/s^2

$\dot{Q}_{H_2O,s}$ Rate of sensible heat transfer of water, kJ/s

$\dot{m}_{H_2O}$ Mass flow rate of water, kg/s

C_{p,H_2O} Specific heat capacity of water, kJ/kg·K

ΔT_{H_2O} Temperature difference between outlet and inlet of water, K

$\dot{Q}_{CO_2,l}$ Rate of latent heat transfer of carbon dioxide, kJ/s

$\dot{m}_{CO_2}$ Mass flow rate of carbon dioxide, kg/s

L_{CO_2} Latent heat of carbon dioxide, kJ/kg

v_{CO_2} Velocity of carbon dioxide, m/s

C_{p,CO_2} Specific heat capacity of carbon dioxide, kJ/kg·K

ρ_{CO_2} Carbon dioxide density, kg/m^3

D_d Diameter at diverging section, m

D_t Diameter at throat section, m

CHAPTER I

INTRODUCTION

1.1 Background

Nowadays, the world is facing overwhelming CO_2 pollution from human daily activities, such as fossil fuel combustion, which is the main cause of greenhouse effect or global warming. So, CO_2 pollution should be reduced or utilized to mitigate the greenhouse effect.

As a sustainable and environmentally friendly concept, ice is used in the preservation of fresh goods as well as in fishing boats. A significant amount of ice is usually required to maintain a constant low temperature when preserving fishing products offshore. To get to this point, a great volume of ice must be carried on fishing boats, which consume a lot of fuel and are therefore a cost to the fishing business and a pollution to the environment, which leads to a CO_2 pollution problem. Thus, improving the quality of ice products should be conducted to lower the load of ice on fishing boats.

Generally, the quality of ice products is based on several properties of raw water, such as cleanliness, contamination, and odor. However, the attributes described above are concerned with quality in terms of food and beverage products. Additionally, there are several properties of ice which are related to physical properties, such as density and solubility of air, as well as latent heat of fusion. Technically, the physical property of water is essential in terms of enhancing the ice product's quality in terms of its function, such as appearance, melting resistance, heat capacity, and prolonged usage. Thus, the study of the physical properties of water enables us to improve the properties of ice products and to provide a unique design for ice production based on a sustainable concept.

Additionally, one of the disadvantages of ice production is the presence of typical dissolved air in water. During the chilling and freezing processes, trapped air usually appears as tiny bubbles inside the ice product, resulting in decreased melting resistance. Thus, air degassing would be referred to as raw water treatment prior to chilling and freezing. It is possible to accomplish this through a vacuum, which is related to Henry's law. It includes a variety of alternatives for generating a vacuum condition, such as the vacuum pump and the venturi effect.

The Venturi jet effect is a phenomenon that occurs when a fluid is forced through a narrow throat. In this study, carbon dioxide is used as a sustainable and environmentally friendly concept. Additionally, the utilization of CO_2, as an enormous pollution, which is an abundant resource, has become increasingly useful and applicable.

1.2 Objectives

1.2.1 To study and develop a water treatment process for improving the quality of water to produce high melting resistance ice via CO_2 utilization.

1.2.2 To investigate the effects of CO_2 supply conditions on the involved parameters of the treatment process.

1.3 Scopes of Work

1.3.1 Develop the water treatment process to improve the quality of water to produce high melting resistance ice by using vacuum degassing and chilling of water via CO_2 utilization.

1.3.2 Analyze the effects of the supply CO_2 temperature and pressure on the vacuum pressure level and outlet water temperature and on the quality of treated water.

1.3.3 Analyze the quality of treated water compared with untreated water via the melting rate of ice.

1.4 Project Outputs

1.4.1 To be able to generate a prototype of the water treatment process via CO_2 utilization which involves the degassing unit and water-pre-cooling unit.

1.4.2 To be able to improve the quality of water after the treatment process.

1.4.3 To be able to identify the parameters of CO_2 supply which influence the performance of the treatment process and the quality of treated water.

CHAPTER II

LITERATURE REVIEW

2.1 General knowledge and phase diagram of carbon dioxide

2.1.1 Carbon dioxide

In the gas phase, carbon dioxide is a non-reactive, non-toxic, and non-corrosive gas. It is a colorless gas that is heavier than air. In general, the air has a low concentration of carbon dioxide that is not harmful. But it will be toxic when the concentration exceeds 5%v/v due to the lag of oxygen. It will lead to headaches, dizziness, high heart rate, and unconsciousness (AirLiquide. 2016).

2.1.2 Liquid carbon dioxide

Carbon dioxide is liquefied by pressure to a range between the triple point and the critical point, with a corresponding temperature range. Liquid carbon dioxide is a volatile substance, and it has a latent heat of vaporization of about 230.5 kJ/kg. So, it is useful in the refrigeration of food production (Span and Wagner. 1994).

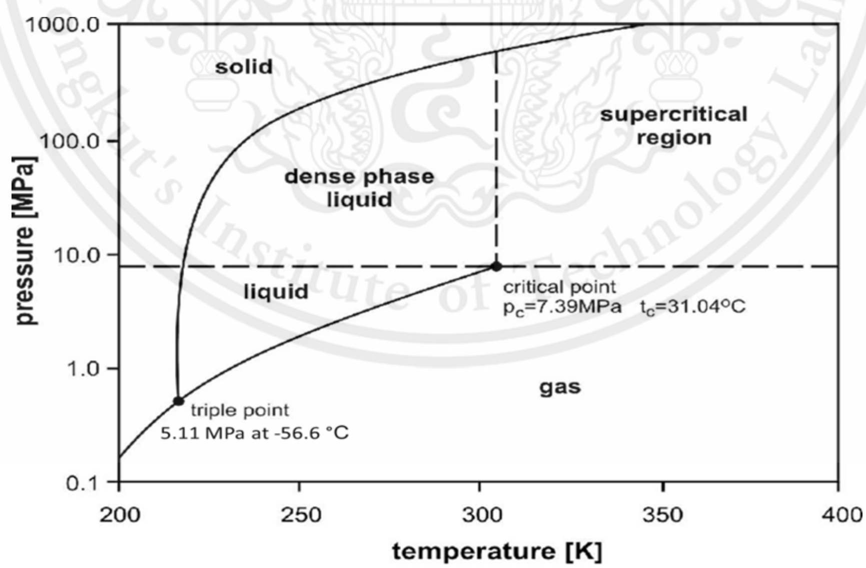

Figure 2.1 Phase diagram of carbon dioxide (Witkowski et al. 2014).

2.1.3 Physical properties of carbon dioxide

The physical properties of carbon dioxide are obtained from "A new equation of state for carbon dioxide covering from the Triple-point temperature to 1100 K at pressures up to 800 MPa" by R. Span and W. Wagner. This work reviews the available data on the thermodynamic properties of carbon dioxide, including density, internal energy, enthalpy, entropy, heat capacity at constant volume, heat capacity at constant pressure, and speed of sound at its extensive temperatures, from triple-point temperature to 1100 K at pressures up to 800 MPa (Span and Wagner. 1994).

2.2 General knowledge of water and air

2.2.1 Water

Water is a transparent, tasteless, odorless, and inorganic substance. Its chemical formula is H_2O. The three common states of H_2O are the liquid phase, solid phase, and gaseous phase, which are called water, ice, and water vapor, respectively. The addition or removal of heat can cause a phase transition, as shown in the figure below (Lumen. 2020).

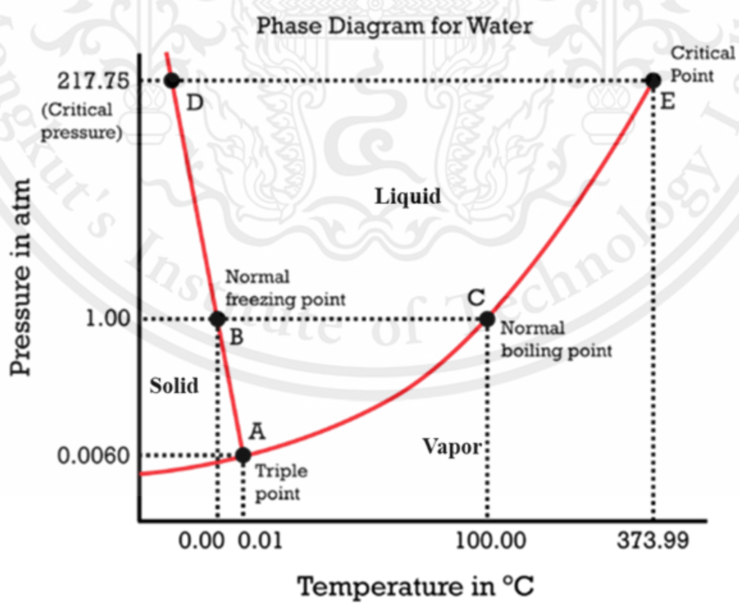

Figure 2.2 Phase diagram of H_2O (Lumen. 2020).

2.2.2 Air

Air is a mixture of various gases that consists of nitrogen, oxygen, noble gases, carbon dioxide, and water vapor. Typically, nitrogen and oxygen are the main components contained in air. In the dry atmosphere, the average mole fraction of nitrogen and oxygen is 0.781 and 0.209, respectively (Lenntech. 2020).

2.3 Vacuum and vacuum degassing

2.3.1 Vacuum

A vacuum is a state of pressure in which the pressure is lower than the atmospheric pressure. A vacuum can be quantitatively defined as the difference between the atmospheric pressure and the pressure in a vacuum system. When the pressure in the vacuum system is close to the atmospheric one, it can be measured by differential manometers that directly measure this difference in pressure (Rozanov. 2002).

2.3.2 Vacuum degassing

Vacuum degassing is used to remove entrapped gases from a liquid. When a vacuum is applied to the surface of the liquid, the gases move to the liquid surface and are drawn out. Similarly, the entrapped gases will also move from high pressure to low pressure by a diffusion process (Sanatron. 2020).

Figure 2.3 Vacuum degassing system (Sanatron. 2020).

2.3.3 Henry's law

Henry's law is used to describe the Vapor/Liquid Equilibrium system (VLE). Henry's law is preferred for dilute concentration conditions of gas in liquid water. It explains that the amount of dissolved gas is proportional to its partial pressure in the gas phase. The proportionality factor is called Henry's constant (Yunus and Michael. 2015).

$$x_i H_i = y_i P_A \tag{2.1}$$

Where x_i= mole fraction of specie i in liquid phase

H_i= Henry's constant, bars

y_i= mole fraction of specie i in vapor phase

P_A=ambient pressure, bars

Table 2.1 Henry's constants for gases dissolved in water at 25°C (Yunus and Michael. 2015).

Gas	**H (bars)**
Acetylene	1,350
Air	72,950
Carbon dioxide	1,670
Carbon monoxide	54,600
Ethane	30,600
Ethylene	11,550
Helium	126,600
Hydrogen	71,600
Hydrogen sulfide	550
Methane	41,850
Nitrogen	87,650
Oxygen	44,380

2.4 Compressible flow

Compressible flow is a flow phenomenon in which the density of fluid significantly changes in response to a change in pressure. This phenomenon can be based on gas flow through an area that gradually decreases and then gradually increases, such as a nozzle. The flow can be treated as compressible when the proportionality between the flow velocity and the speed of sound exceeds 0.3 and the proportionality is called the Mach number. Moreover, the compressible flow can be divided by Mach number, including subsonic when Ma < 1, sonic when Ma = 1, and supersonic when Ma > 1. For sonic flow at Ma = 1, it is called a critical condition (Yunus and Michael. 2015).

$$Ma=\frac{v}{c} \tag{2.2}$$

Where c = speed of sound, m/s

Ma = Mach number

v = fluid flow velocity, m/s

2.4.1 Isentropic flow through nozzle

The background of ideal venturi nozzle design, one-dimensional isentropic flow, and ideal gas are always applied. So, the list of equations below and Table 2.2 can be applied to design a venturi nozzle which is respected by the Mach number (Yunus and Michael. 2015).

$$\frac{T_{CO_2}}{T_{CO_2,0}}=\left(1+\frac{k-1}{2}Ma^2\right)^{-1} \tag{2.3}$$

$$\frac{P_{CO_2}}{P_{CO_2,0}}=\left(1+\frac{k-1}{2}Ma^2\right)^{-k/(k-1)} \tag{2.4}$$

$$\frac{A}{A^*}=\frac{1}{Ma}\left[\left(\frac{2}{k+1}\right)\left(1+\frac{k-1}{2}Ma^2\right)\right]^{\frac{0.5(k+1)}{(k-1)}} \tag{2.5}$$

Where Ma = Mach number

T_{CO_2}= local temperature of carbon dioxide, K

$T_{CO_2,0}$ =inlet temperature of carbon dioxide, K

P_{CO_2}= local pressure of carbon dioxide, bars

$P_{CO_2,0}$=inlet pressure of carbon dioxide, bars

A= local cross-sectional area, m^2

A^*= cross-sectional area at throat, m^2

k = heat capacity ratio

Table 2.2 One-dimensional isentropic compressible-flow functions for an ideal gas with k=1.28 (Carbon dioxide) (Yunus and Michael. 2015).

Ma	**A/A^***	**$P_{CO_2}/P_{CO_2,0}$**	**$T_{CO_2}/T_{CO_2,0}$**
0.00	∞	1.00	1.00
0.10	5.90	0.99	0.99
0.20	3.00	0.98	0.99
0.30	2.06	0.94	0.99
0.40	1.60	0.90	0.98
0.50	1.35	0.85	0.97
0.60	1.19	0.80	0.95
0.70	1.10	0.74	0.94
0.80	1.04	0.68	0.92
0.90	1.01	0.61	0.90
1.00	1.00	0.55	0.88
1.20	1.03	0.43	0.83
1.40	1.12	0.33	0.79
1.60	1.28	0.25	0.74
1.80	1.49	0.18	0.69
2.00	1.79	0.13	0.64
2.20	2.19	0.09	0.60
2.40	2.71	0.07	0.55

2.4.2 Variations of subsonic and supersonic flow with flow area

The increase or decrease in pressure and Mach number when passing through gradually increases or decreases in flow area and depends on the inlet Mach number. This relationship can be explained by the below equation, which is summarized in Figure 2.4 (Yunus and Michael. 2015).

$$\frac{dA}{A} = -\frac{dv}{v}\left(1 - Ma^2\right) \tag{2.6}$$

Where A = cross sectional area, m^2

v= flow velocity, m/s

Ma= Mach number

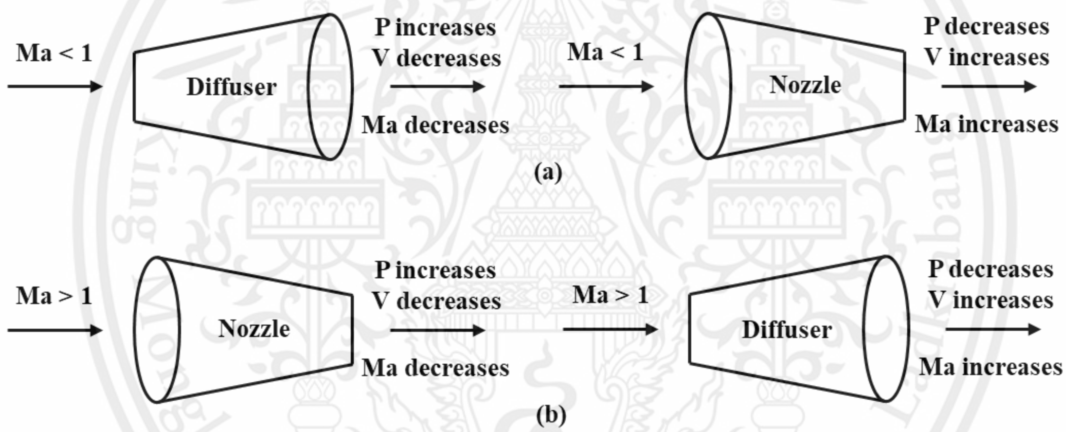

Figure 2.4 Variations of subsonic (a) and supersonic (b) flow through nozzle and diffuser (Yunus and Michael. 2015).

2.5 Bernoulli's principle

Bernoulli's equation is considered an incompressible fluid in a pipe that varies in cross-section area and height. This equation is a principle of conservation of energy for frictionless laminar flow which describes the relationship between pressure and flow velocity (Yunus and Michael. 2015).

$$P_{H_2O,I}+\frac{1}{2}\rho_{H_2O}v^2_{H_2O,I}+\rho_{H_2O}gh_{H_2O,I}=P_{H_2O,O}+\frac{1}{2}\rho_{H_2O}v^2_{H_2O,O}+\rho_{H_2O}gh_{H_2O,O} \quad (2.7)$$

Where $P_{H_2O,I}$ = Inlet pressure of water, kPa

$v_{H_2O,I}$,= Inlet velocity of water, m/s

$h_{H_2O,I}$ = Inlet height of water from the reference point, m

$P_{H_2O,O}$ = Outlet pressure of water, kPa

$v_{H_2O,O}$ = Outlet velocity of water, m/s

$h_{H_2O,O}$ = Outlet height of water from reference point, m

ρ_{H_2O} = Density of water, kg/m^3

g = Gravitational constant, m/s^2

2.6 Heat transfer

Heat is the form of energy that can be transferred from one system to another because of the temperature difference, and thermal energy is always transferred from a hot object to a cold object. Moreover, the amount of heat loss from a hot object is always equal to the heat received by a cold object (Yunus and Afshin. 2015).

2.6.1 Sensible heat of water

Sensible heat is the amount of heat transferred without any phase change processes and its equation is shown below (Yunus and Afshin. 2015).

$$\dot{Q}_{H_2O,s}=\dot{m}_{H_2O}C_{p,H_2O}\Delta T_{H_2O} \tag{2.8}$$

Where $\dot{Q}_{H_2O,s}$ = Rate of sensible heat of water, kJ/s

$\dot{m}_{H_2O}$ = Mass flow rate of water, kg/s

C_{p,H_2O} = Specific heat capacity of water, kJ/kg·K

ΔT_{H_2O} = Temperature difference between outlet and inlet of water, K

2.6.2 Latent heat of carbon dioxide

Latent heat is the amount of heat transferred with phase change processes and its equation is shown below (Yunus and Afshin. 2015).

$$\dot{Q}_{CO_2,l}=\dot{m}_{CO_2}L_{CO_2} \tag{2.9}$$

Where $\dot{Q}_{CO_2,l}$ = rate of latent heat transfer of carbon dioxide, kJ/s

$\dot{m}_{CO_2}$ = mass flow rate of carbon dioxide, kg/s

L_{CO_2} = latent heat of carbon dioxide, kJ/kg

2.7 Check valve

A check valve is a valve that allows fluid to flow in one direction. Check valves work automatically when the difference between upstream pressure and downstream pressure is higher than the cracking pressure. For vacuum system design, the important problem is water flow into vacuum equipment because of the differential pressure between the vacuum side and the atmospheric side. Therefore, a check valve can be used to eliminate the effect of atmospheric pressure by using the seal on the check valve.

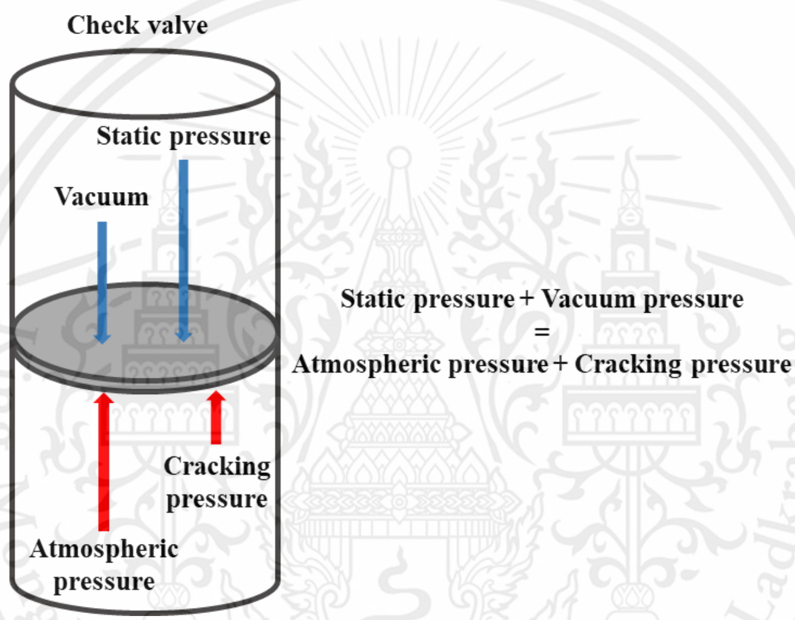

Figure 2.5 Check valve pressure balance.

CHAPTER III

RESEARCH METHODOLOGY

3.1 Chemicals and equipment

1. Reverse osmosis water
2. 99.5% purity carbon dioxide
3. CONCOA pressure regulator
4. Analog pressure gauge
5. KITA digital vacuum gauge
6. Capital vacuum pump VE115 model
7. Swagelok check valve CH series at given cracking pressure of 1/3 psi
8. Water trap separator
9. Swagelok tube fittings
10. Type K thermocouple
11. Wisco AI210 Datalogger
12. 2.5 centimeters diameter plastic ice mold
13. Refrigerator
14. Mettler Toledo XS32001L XS Top loading Balance with RS 232 cable
15. Plastic funnel
16. Three-dimensional printer Anet a8 model
17. Polyethylene terephthalate glycol (PETG) filament 1.75 mm
18. Thread tap

3.2 Conceptual design

The objectives of this design are the elimination of dissolved air from water by vacuum and pre-cooling of water with carbon dioxide before the freezing process. The figure below shows the conceptual design. Firstly, water is pulled into the vacuum chamber for degassing by a vacuum force and drops into the evaporator for pre-cooling. For liquid carbon dioxide, the difference in temperature between water and liquid carbon dioxide can cause an evaporation process of liquid carbon dioxide. Thus, liquid carbon dioxide flows to the evaporator, where it is converted to a gas before entering a venturi nozzle to create a vacuum. For a vacuum pump, the pump is used to fill the water in the system at the beginning.

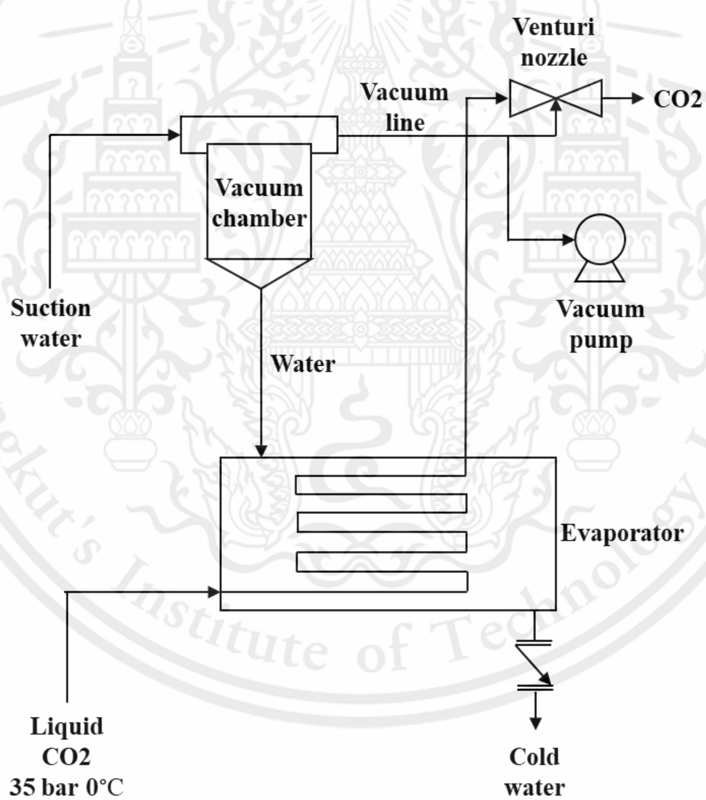

Figure 3.1 Conceptual design of the device.

3.3 Procedure

3.3.1 Venturi nozzle design

Assume a constant temperature of 0 °C because of the phase change process.

1. Read the pressure ratio and temperature ratio at Ma = 1 from Table 2.2.

2. Calculated critical pressure and critical temperature from equations 2.3 and 2.4.

3. Calculated critical velocity from the below equation by substituting critical temperature.

$$v_{CO_2}=\sqrt{2C_{pCO_2}\left(T_{CO_2,0}-T_{CO_2}\right)} \tag{3.1}$$

Where v_{CO_2}= throat velocity of carbon dioxide, m/s

C_{p,CO_2}= specific heat capacity of carbon dioxide, kJ/kg·K

$T_{CO_2,0}$ = inlet temperature of carbon dioxide, K

T_{CO_2}= local temperature of carbon dioxide, K

4. Calculated the throat area from the below equation with a mass flow rate of about 5 g/s.

$$A^*=\frac{\dot{m}_{CO_2}}{\rho_{CO_2}v_{CO_2}} \tag{3.2}$$

Where A^*= throat area, m^2

$\dot{m}_{CO_2}$= carbon dioxide mass flow rate, kg/s

ρ_{CO_2}= carbon dioxide density, kg/m^3

v_{CO_2}= throat velocity of carbon dioxide, m/s

5. Defined vacuum pressure and substituted critical pressure in equation 2.4 to calculate Mach number at the diverging section.

6. Calculated outlet area by substituting exit Mach number and throat area in equation 2.5.

7. Calculated diameter at each section from cross-section area and made a ratio between diameter at the throat section and diverging section to upscale because a very small diameter could easily lead to blockage at the throat and limitation of equipment**.**

8. Draw the designed venturi nozzle in Tinkercad software with recommended converging and diverging angles of 45° and between 8° to 12° respectively (Singh et al. 2019).

9. Printed the designed venturi nozzle with a three-dimensional printer.

10. The nozzle was taped with thread tap.

3.3.2 Venturi nozzle test

1. Connected the designed venturi nozzle with a carbon dioxide gas cylinder.

2. Connected the suction port of the venturi nozzle with a vacuum chamber that installed a digital vacuum gauge.

3. Open the gas cylinder valve, then set the pressure regulator to the calculated pressure.

4. Recorded video with a camera phone.

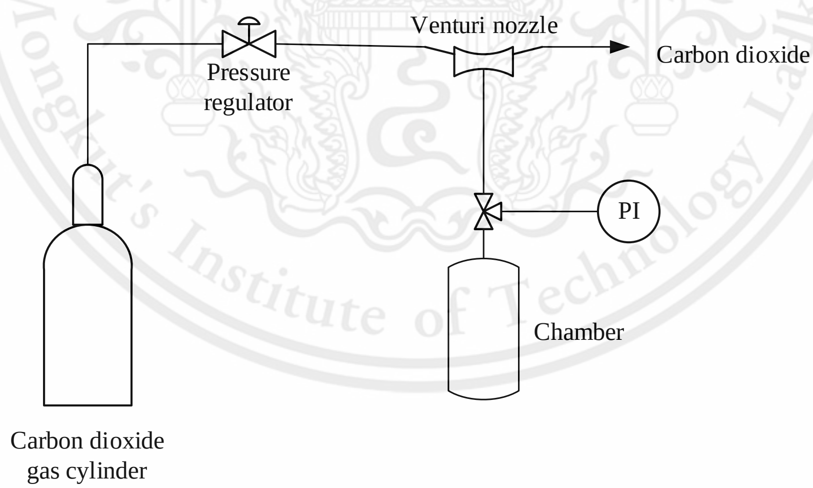

Figure 3.2 venturi nozzle test.

3.3.3 Vacuum system design

1. Calculated the relationship between vacuum pressure and the required height of the system to open the 1/3 psi check valve and water outlet flow rate by Bernoulli's equation.

2. Assemble the Swagelok fitting and measure the system's height.

3. Compare the height of the system with the previous calculation to find the maximum vacuum pressure for the designed system.

4. If productivity is too low, a pump should be installed at the water outlet.

Table 3.1 System height with maximum vacuum pressure.

System height (m)	Static pressure (kPa)	Vacuum pressure (kPa)	System height (m)	Static pressure (kPa)	Vacuum pressure (kPa)
0.10	0.98	-1.32	1.10	10.79	8.49
0.20	1.96	-0.33	1.20	11.77	9.48
0.30	2.94	0.65	1.30	12.75	10.46
0.40	3.92	1.63	1.40	13.73	11.44
0.50	4.91	2.61	1.50	14.72	12.42
0.60	5.89	3.59	1.60	15.70	13.40
0.70	6.87	4.57	1.70	16.68	14.38
0.80	7.85	5.55	1.80	17.66	15.36
0.90	8.83	6.53	1.90	18.64	16.34
1.00	9.81	7.51	2.00	19.62	17.32

3.3.4 Ice melting test

1. Set the chamber on the Mettler Toledo XS32001L XS Top loading Balance.

2. Place a 250 ml flask inside the chamber.

3. Set LabX direct balance 2.5 software on the computer, then connect RS232 to the computer and set the balance to continuous mode.

4. Set a thermometer to see the temperature during the experiment.

5. Set a plastic funnel with a clamp inside the chamber without contact between the chamber and the clamp.

6. Placed ice in a plastic funnel, then set zero on the balance and started the record.

7. Plotted graph mass varies with time, then find the slope of the graph.

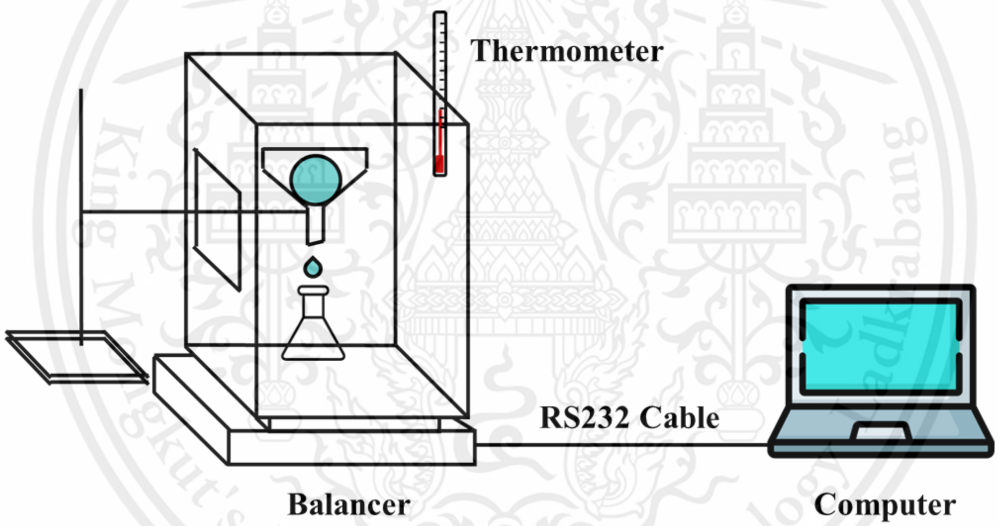

Figure 3.3 Ice melting test setup.

3.3.5 Heat exchanger section design

1. Calculated the amount of required heat to evaporate liquid carbon dioxide from equation 2.9.

2. Calculated amount of required water flow rate from equation 2.8

CHAPTER IV

RESULTS AND DISCUSSION

4.1 Design of overall system

Most of the components in this project were received from unused fittings and equipment in the project room. As a result, several defects will be present. The overall system in this project could be divided into three main parts, including the vacuum system, heat exchanger, and liquid carbon dioxide source, as shown in the further topics.

4.1.1 Design of vacuum system

In this project, water had to be treated by vacuum degassing. The water overflowed into the vacuum pump or venturi nozzle, which was the main issue with the design. This problem could be solved by installing a 1/3 psi check valve at the exit of the system to eliminate the effect of the difference between atmospheric pressure and system pressure. A ball valve was also installed after the check valve for smoother operation at the start of the operation. In addition, the water trap separator was considered because it had enough connection ports and had a complex flow way design with a water filter trap, as shown in Figure 4.1. As the calculation shown in Appendix B.2 and the experiment results show in Appendix B.6, the productivity of this system would be very low if only static pressure were applied. So, to achieve more productivity, a pump was installed at the water outlet of the system. To supply water, water is transferred to the system through a submerged flexible tube in the water storage tank by vacuum.

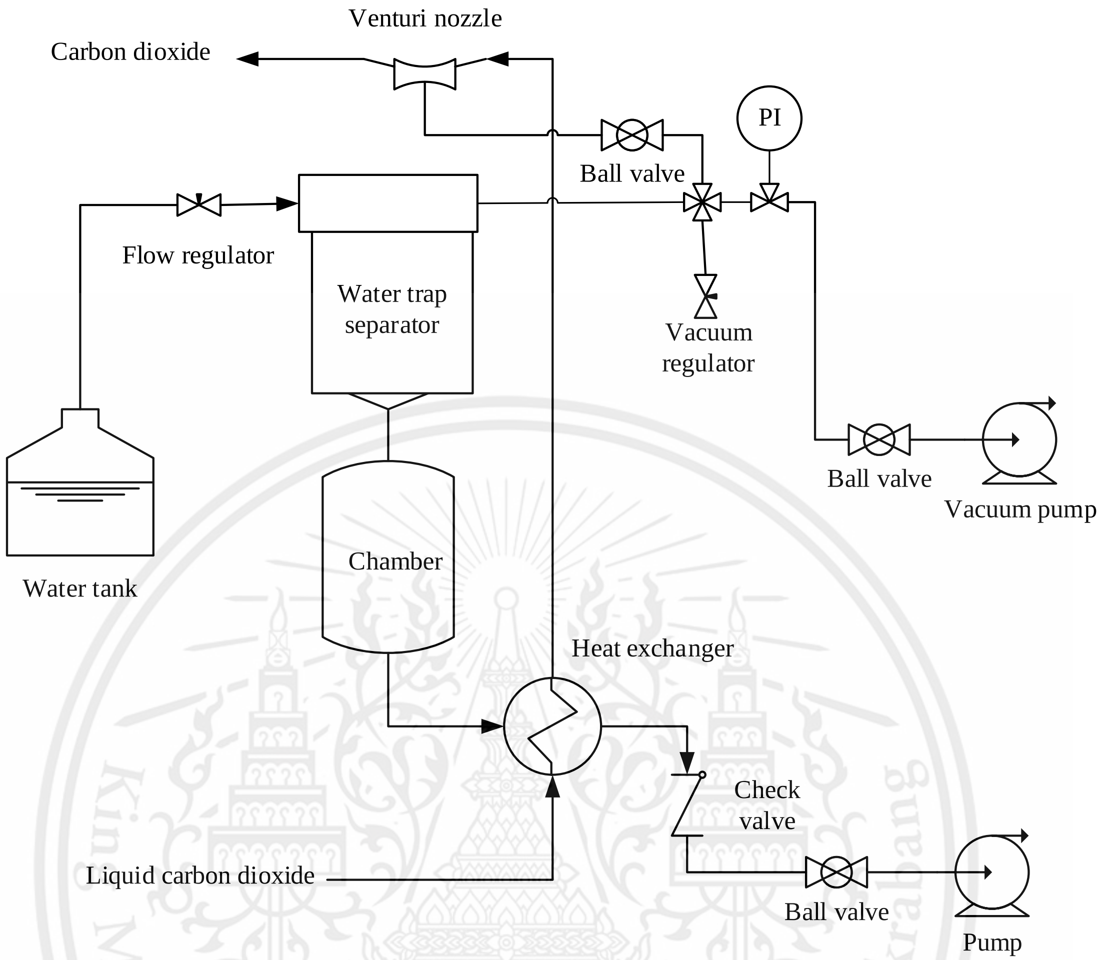

Figure 4.1 Vacuum system and components.

But in this prototype, many defects were identified, including the narrow throat between the water trap separator and another chamber and the unequal size between the inlet diameter of the pump and the tube of the system. For the narrow throat, it could cause a lack of water flow in the system because of more suction force in a smaller space compared with the space of the water trap separator. Lastly, the defect of unequal size at the pump inlet led to low efficiency of the pump due to the inlet pump having a fraction of air.

4.1.2 Design of heat exchanger system

To ensure phase of carbon dioxide, a double-pipe heat exchanger was modified by installing two four-way fittings to install pressure gauges and type-K thermocouples with a temperature range between -200 °C to 1250 °C at each four-way fitting as shown below. All pressure gauges and thermocouples allow us to monitor inlet and outlet conditions at the carbon dioxide pipe. The materials of the double-pipe heat exchanger were a copper tube for the inner tube and an insulated stainless-steel tube for the outer tube with an approximate length of 180 centimeters.

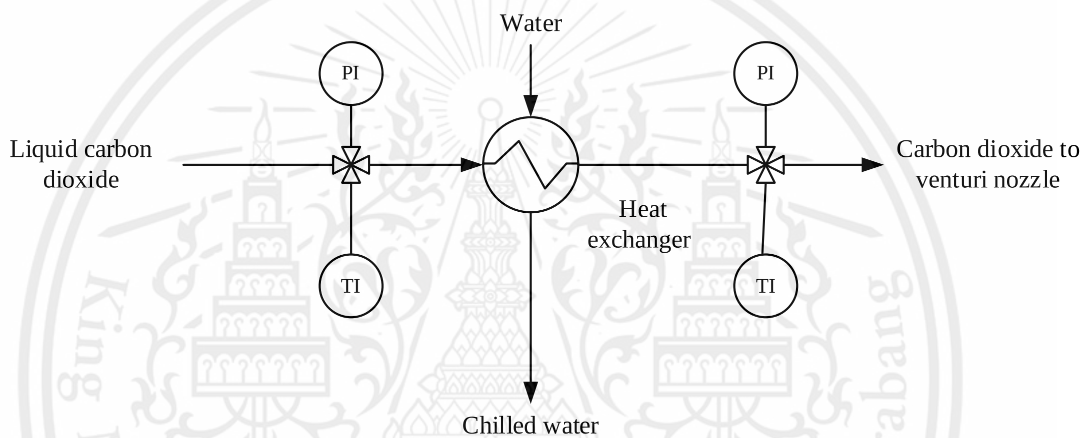

Figure 4.2 Heat exchanger system and components.

4.1.3 Liquid carbon dioxide source

Liquid carbon dioxide could be done by increasing pressure higher than 5.17 bars and decreasing temperature. In this project, liquid carbon dioxide was provided by modifying a dry ice cleaning machine. This dry ice cleaning machine had a temperature control system in a liquid carbon dioxide chamber with pressure from a carbon dioxide gas cylinder. So, carbon dioxide was liquefied by reducing the temperature to 0 °C at a pressure of 40 bars. For modification of the machine, the liquid carbon dioxide tube that directly connects to the liquid carbon dioxide chamber of the dry ice cleaning machine was cut and replaced with a three-way fitting. Then, connect to the system as shown in Figure 4.3 with a ball valve for on-off function and connect to the heat exchanger.

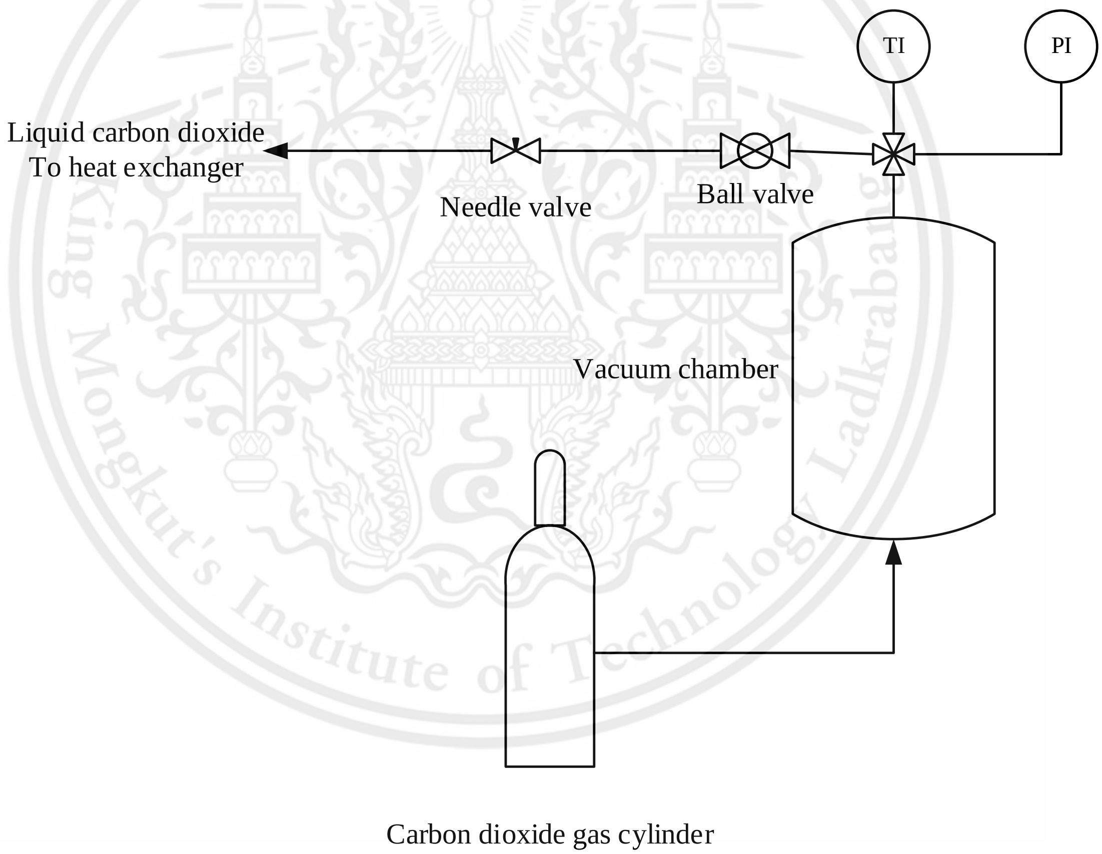

Figure 4.3 Liquid carbon dioxide source and components.

4.2 Startup procedure

1. Turn on the vacuum pump to fill the water and eliminate air in the system by adjusting the vacuum regulating valve.

2. Turn off the vacuum pump and turn on the ball valve at the water outlet to fill the water into the water pump inlet, then close the ball valve.

3. Fully closed vacuum regulator and gradually opens liquid carbon dioxide needle valve.

4. Adjusting vacuum pressure by adjusting the vacuum regulates the valve.

5. Open the water outlet ball valve and turn on the water pump, then balance the level of water by observing the level of the water trap separator.

6. Fill water in an ice mold, then place the mold in the freezer.

4.3 Nozzle dimension and vacuum pressure

The Venturi nozzle was designed by using the calculation in Appendix B.3 as a guide. The dimensions of the nozzle are shown in the figure below.

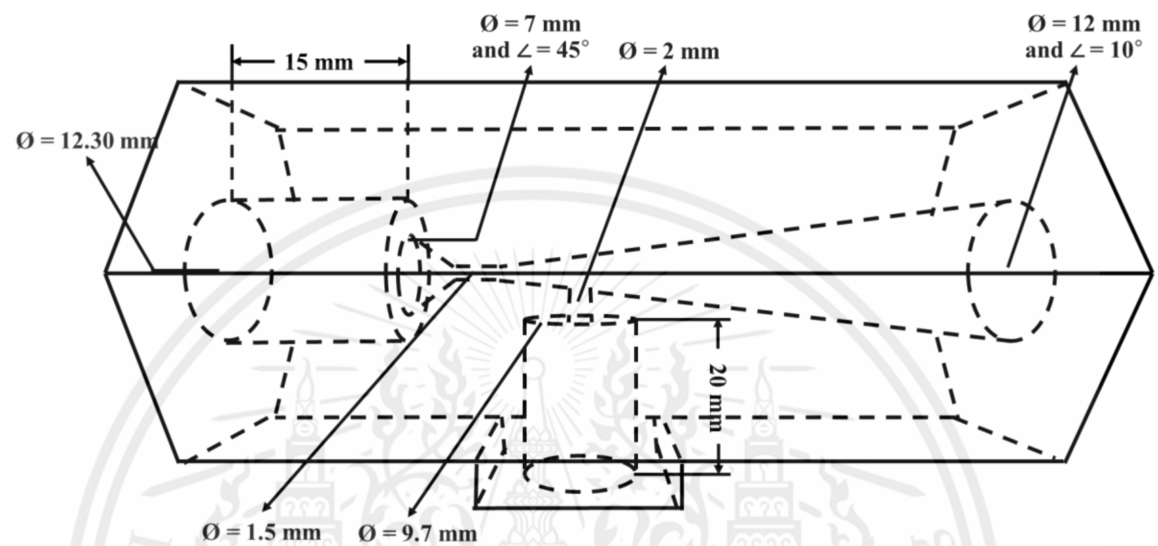

Figure 4.4 Nozzle geometry.

This nozzle must be connected to the system by 1⁄4" union male connector at a port diameter of 12.30 mm for carbon dioxide flow and connected by a 1/8" union male connector at a port diameter of 9.7 mm for suction air in the system. Moreover, the vacuum pressure at 30 bars of inlet pressure was 77.6 kPa, as shown in Figures B.5.1 in Appendix B.5.

4.4 Overall results

On this topic, the condition of the system and the ice melting rate were examined and discussed. The test case for normal reverse osmosis water was named NorRO. For named treated water, 5APR, 6APR, and 7APR were used.

4.4.1 Conditions of water and carbon dioxide at heat exchanger

The temperature of the water outlet is determined by the mass flow rate of liquid carbon dioxide and the residence time of water. The different temperatures of pre-treatment and post-treatment of water were examined by a type-K thermocouple. For carbon dioxide, the condition of carbon dioxide was measured by two analog pressure gauges and two thermocouples type-K.

The results of the pressure and temperature of carbon dioxide and water are shown in Table 4.1. For carbon dioxide, first, liquid carbon dioxide at 40 bars and 0 °C is fed and passed through a needle valve that creates Joule-Thomson effects. For 6APR, liquid carbon dioxide did not exist due to unsuitable conditions at -26.3 °C and 12 bars. So, the different temperatures of water were not too much, and a vacuum pressure of 87.6 kPa was achieved. On 7APR, carbon dioxide was in a mixture between the liquid phase and the gas phase at -18.5 °C and 20 bars. That could be noticed because the temperature change in the water was larger than in the 6APR case. From both previous results, the experiments were done on the counter-current flow of the double-pipe heat exchanger. There is a water freezing problem due to the Joule-Thomson effect. So, too much energy was absorbed by liquid carbon dioxide around the needle valve. To solve this problem, the mass flow rate of water will be increased. But at the pump, it had another problem, as mentioned in the design of vacuum system topic. In addition, the co-current flow state would solve this problem because the temperature difference is smaller than the counter-current flow state through the system when compared with the counter-current flow at the needle valve.

Table 4.1 Conditions of water and carbon dioxide.

Tests	CO_2 Pressure (bars)		CO_2 Temperature (°C)		Water Temperature (°C)		Water flow rate (ml/s)	Vacuum pressure (kPa)
	Inlet	Outlet	Inlet	Outlet	Inlet	outlet		
6APR	12	11.83	-26.3	9.9	26.0	16.8	7.62	87.62
7APR	20	19.61	-18.5	23.3	26.0	11.4	8.12	90.22

4.4.2 Air solubility at various vacuum pressure

The result of air solubility or the mole fraction of air in water is shown in Table 4.2 and Figure 4.5. According to Henry's law, air solubility in water will be reduced in vacuum conditions when compared with atmospheric pressure. In Table 4.2, the mole fraction of air in water was calculated. But this calculation would be true when the degassing step reaches an equilibrium that needs more study for better performance.

Table 4.2 Air solubility at various vacuum pressure.

Tests	Vacuum pressure (kPa)	Mole fraction of air in water
NorRO	101.32	1.39×10^{-5}
5APR	89.72	1.23×10^{-5}
6APR	87.62	1.20×10^{-5}
7APR	90.22	1.24×10^{-5}

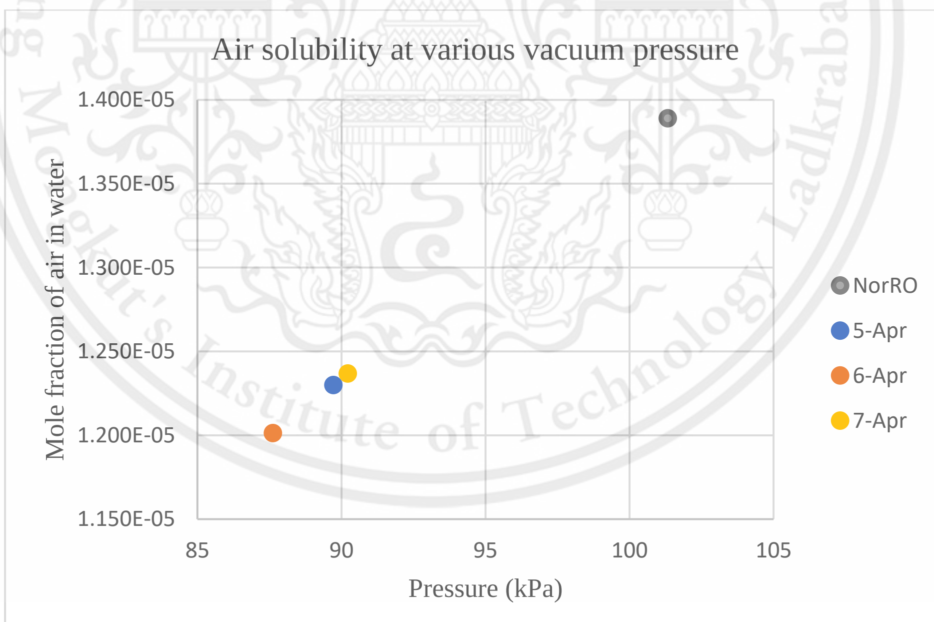

Figure 4.5 Air solubility at various vacuum pressure.

4.4.3 Effect of liquid carbon dioxide mass flow rate on different water temperature

Liquid carbon dioxide was the cooling working fluid in this work. A higher liquid carbon dioxide mass flow rate would cause a greater difference in the temperature of the water between the inlet and outlet. The mass flow rate of liquid carbon dioxide would be varied in this topic to investigate the temperature change of existing water. The mass flow rate of water and the specific heat capacity of water were fixed at 8.0×10^{-3} kg/s and 4.18 kJ/kg·K, respectively. According to the CO_2 phase diagram, liquid carbon dioxide was assumed to be saturated liquid at a pressure of 35 bars and 0 °C and only a phase change process occurred. The assumptions for this topic were that heat absorbed equals heat released and an efficient heat exchanger. The resulting graph is shown below, and the calculation can be found in Appendix B.4.

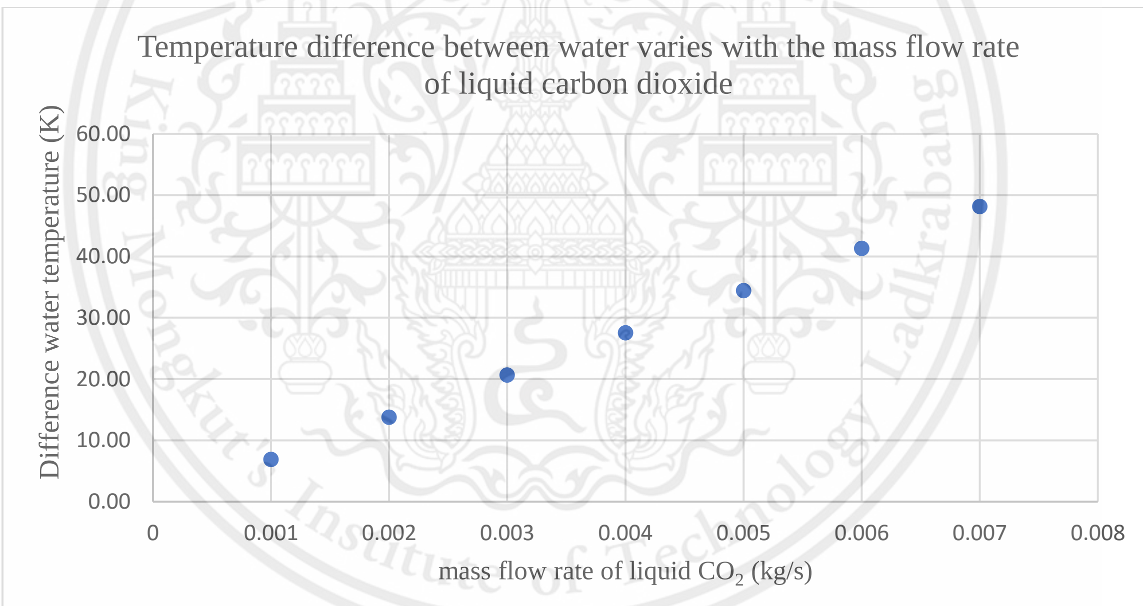

Figure 4.6 Temperature difference between water varies with the mass flow rate of liquid carbon dioxide.

In Figure 4.6, the result shows a linear relationship because of the assumptions. But in practice, the difference in temperature would not exceed the initial temperature of the water because it would freeze. But this graph would guide us to the maximum flow rate of carbon dioxide and the maximum water temperature change.

4.4.4 Melting rate of ice from treated water raw source at any temperature and vacuum pressure treatments

The result of the melting rate of ice in various treatment conditions is shown in Table 4.3 and Figure 4.8. An example of the ice appearance was shown in Figure 4.7, which appears to be a round shape and have air bubbles inside the ice ball.

Figure 4.7 Ice ball appearance.

As shown in Table 4.3, the melting rate of ice decreased from 2.8×10^{-3} g/s for normal reverse osmosis water after the treatments to 2.7×10^{-3} g/s for treatment conditions at 87.6 kPa for degassing and 16.8 °C for pre-cooling. But the melting rate was decreased further to 2.5×10^{-3} g/s at treatment conditions of 89.7 kPa for degassing and 11.5 °C for pre-cooling and 2.4×10^{-3} g/s at treatment conditions of 90.2 kPa for degassing and 9.0 °C for pre-cooling. From the results, the trend of vacuum pressure and outlet temperature had the opposite trend, which may be the result of a difference in mass flow rate between the gas phase and liquid phase, because in the 7APR case, the phase of carbon dioxide at the inlet heat exchanger tends to have a liquid phase that has a large difference in density when compared with the 6APR case, where the inlet phase was the gas phase. It may be concluded that degassing is not the main treatment to enhance ice melting resistance, as shown in Table 4.3. But the enhancement of the resistance was achieved by the pre-cooling of water under vacuum conditions for this work.

Table 4.3 Melting rate of ice of various treated water.

Tests	Treated water condition		Melting rate (g/s)	Ambient temperature for melting (°C)
	Outlet temperature (°C)	Vacuum pressure (kPa)		
NorRO	26.0	101.325	2.8×10^{-3}	26.0
5APR	11.5	89.725	2.5×10^{-3}	26.0
6APR	16.8	87.625	2.7×10^{-3}	26.0
7APR	9.0	90.225	2.4×10^{-3}	26.0

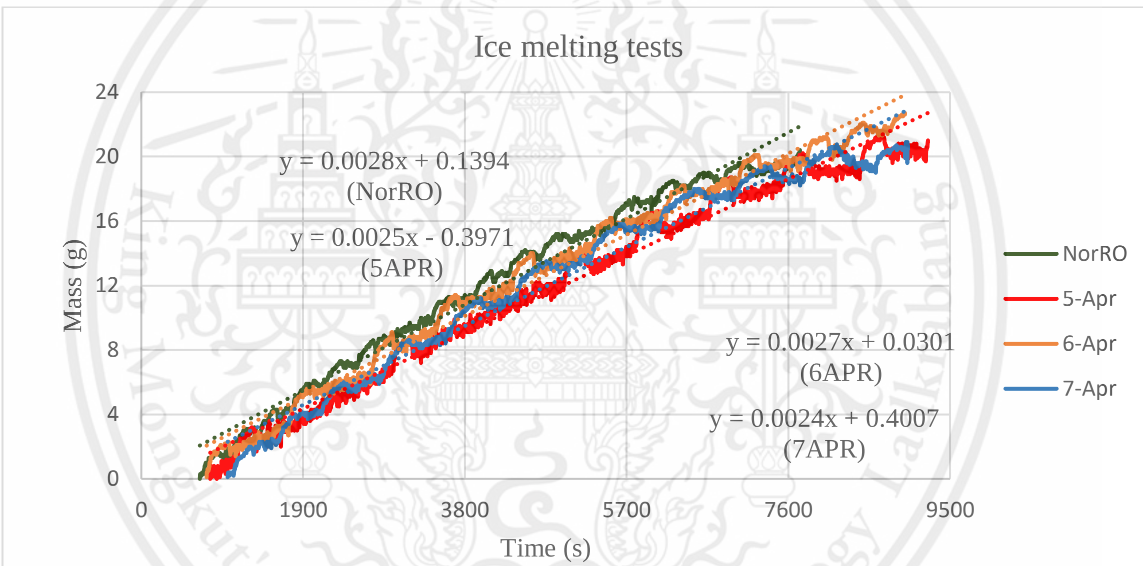

Figure 4.8 Ice melting tests for any cases.

For more easily seen differences between the melting behavior of ice from untreated water cases and treated water cases, the NorRO case and 7APR case were used as representatives of this explanation. From Figure 4.9, mentioned before, the melting rate of the 7APR case was lower than the NorRO case. But the onset of the melting process in the 7APR case was higher than in the NorRO case. Moreover, the final mass of the 7APR case was higher than the final mass of the NorRO case. It may be concluded that the enhancement of the resistance was achieved by observing the different onset and final mass of ice.

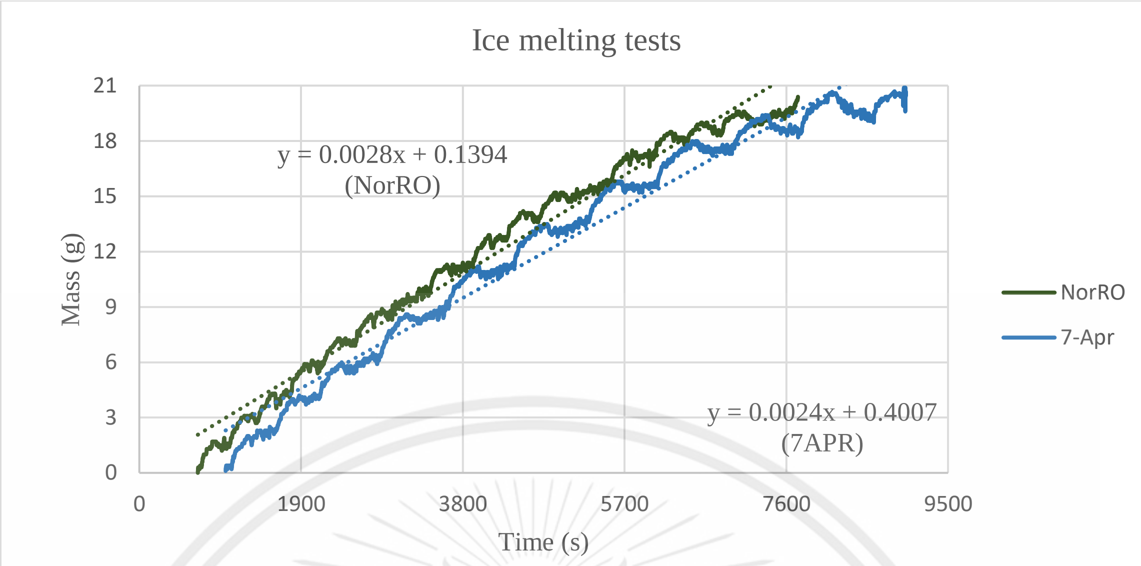

Figure 4.9 Ice melting test of NorRO case and 7APR case.

CHAPTER V

CONCLUSION

5.1 Conclusion

This work provides the application of carbon dioxide utilization to improve and treat water for ice production. CO_2 is used as a working fluid to improve the quality of water by vacuum degassing and pre-cooling for high melting resistance ice production projects. By measuring the melting rate of ice as an indicator of melt resistance, the degassing and pre-cooling system worked successfully in producing high melting resistance ice. For degassing, a venturi nozzle was developed to provide a vacuum condition for degassing which evaporated liquid carbon dioxide and was reused as a working fluid for the nozzle. A cooling system was designed for the water-pre-cooling unit by adapting a double-pipe heat exchanger that functions as an evaporator for phase change of carbon dioxide. After treating water by degassing and pre-cooling, the melting resistance of the ice was enhanced to prolong the ice's lifetime. According to the experimental results, the melting rate of ice was lowered from 2.8×10^{-3} g/s for normal reverse osmosis water (untreated water) to 2.4×10^{-3} g/s after the treatments. Moreover, this work requires additional research and development to correct weaknesses and improve performance, as this work served as a pioneer model for this concept.

5.2 Suggestions

1. The vacuum chamber should be made into one continuous piece to avoid intermittent water flow due to the narrow section at the connector between the two chambers.

2. The diameter size between the pump connector and the stainless-steel tube should be equalized.

3. The mass flow rate of liquid carbon dioxide should be measured during the test.

4. To improve the efficiency of the degassing process, the transfer surface area should be increased by spraying water or another method.

REFERENCES

AirLiquide. 2016. **Safety Data Sheet CARBON DIOXIDE, Compressed & Liquefied Gas**. [Online].Available : http://docs.airliquide.com.au/msdsau/AL062.pdf

Lumen. 2020. **Phase Diagram for Water**. [Online].Available : https://courses.lumenlearning.com/cheminter/chapter/phase-diagram-for-water/

Lenntech. 2020. **FAQ air chemistry and physics Frequently Asked Questions**. [Online].Available : https://www.lenntech.com/faq-air-chemistry-physics.htm

Pratt, J. H. 1932. "Liquid Carbon Dioxide as a Refrigerant." **INDUSTRIAL AND ENGINEERING CHEMISTRY**. 1932(6) : 613–614.

Rozanov, L. N. 2002. **VACUUM TECHNIQUE**. London : Taylor and Francis group.

Sanatron. 2020. **Vacuum Degassing Systems**. [Online].Available : https://www.sanatron.com/vacuum-degassing-systems.php.

Span, R. Wagner, W. 1994. "A New Equation of State for Carbon Dioxide Covering the Fluid Region from the Triple-Point Temperature to 1100 K at Pressures up to 800 MPa." **Journal of Physical and Chemical Reference Data**. 1996 : 1509–1596.

Singh, J. Zerpa, L. E. Partington, B. Gamboa, J. 2019. "Effect of Nozzle Geometry on Critical-Subcritical Flow Transitions." **Heliyon**. 2019(5) : 1-19

Witkowski, A. Majkut, M. Rulik, S. 2014. "Analysis of Pipeline Transportation Systems for Carbon Dioxide Sequestration." **Archives of Thermodynamics**. 2014(*35)* : 117–140.

Yunus A. Cengel, Michael A. Boles. 2015. **Thermodynamics An Engineering Approach**. Eighth. New York : McGraw-Hill Education.

Yunus A. Cengel, Afshin J. Ghajar. 2015. **Heat and Mass Transfer**. Fifth. New York : McGraw-Hill Education.

APPENDIXES

Appendix A Properties of carbon dioxide and water

Appendix B Experimental results and calculations

Appendix B.1 Calculation of maximum percent dissolved air change varies with vacuum pressure.

Appendix B.2 Calculation of outlet flow rate of water of the system without water outlet pump

Appendix B.3 Calculation of nozzle geometry

Appendix B.4 Calculation of the difference in water temperature

Appendix B.5 Vacuum pressure at 30 bars inlet pressure

Appendix B.6 Productivity of the system without pumping at downstream

Appendix A Properties of carbon dioxide and water

Table A.1 Properties of carbon dioxide (Yunus and Michael. 2015).

Temperature (K)	C_p (kJ/kg.K)	Density (kg/m^3)
253.647	1.298	52.540
255	1.277	51.941
260	1.213	49.914
265	1.165	48.129
270	1.128	46.533
275	1.099	45.090
280	1.076	43.772
285	1.057	42.560
290	1.043	41.438

Table A.2 Properties of water (Yunus and Michael. 2015).

Temperature (°C)	C_p (kJ/kg.K)	Density (kg/m^3)
0.01	4.22	1000.00
5	4.21	1000.00
10	4.20	1000.00
15	4.19	999.00
20	4.18	998.00
25	4.18	997.00
30	4.18	996.00
35	4.18	994.00
40	4.18	992.10
45	4.18	990.10
50	4.18	988.10

Appendix B: Experimental results and calculations

Appendix B.1 Calculation of maximum percent dissolved air change varies with vacuum pressure

Calculation of maximum dissolved air in water with vacuum pressure

$$x_iH_i = y_iP_A$$

Where x_i = Mole fraction of specie i in liquid phase

H_i = Henry's constant, bars

y_i = Mole fraction of specie i in vapor phase

P_A = Ambient pressure, bars

Example calculation of maximum dissolved air in water with vacuum pressure

Where H = 72,950 bars

$y_i = 1$

P = 0.91325 bars

$x_iH_I = y_iP$

$x\times(72{,}950\text{kPa}) = 1\times0.91325\text{kPa}$

$x = 1.252\times 10^{-5}$

Calculation of maximum percent dissolved air in water change with vacuum pressure

$$\%\Delta x = \left(\frac{x_{atm}-x}{x_{atm}}\right)\times 100\%$$

Where $\%\Delta x$ = Percent dissolved air in water change, %

x_{atm} = Mole fraction of dissolved air in water at 1 atm

x = Mole fraction of dissolved air in water vary with vacuum pressure

Example calculation of maximum percent dissolved air in water change with vacuum pressure

Where $x_{atm} = 1.39\times 10^{-5}$

$x = 1.252\times 10^{-5}$

$$\%\Delta x = \left(\frac{(1.39\times10^{-5})-(1.252\times10^{-5})}{(1.39\times10^{-5})}\right)\times 100\%$$

$\%\Delta x = 9.87\%$

Appendix B.2 Calculation of outlet flow rate of water of the system without water outlet pump

Calculation of outlet water flow rate of the system without water outlet pump

$$P_{H_2O,I}+\frac{1}{2}\rho_{H_2O}v^2_{H_2O,I}+\rho_{H_2O}gh_{H_2O,I} = P_{H_2O,O}+\frac{1}{2}\rho_{H_2O}v^2_{H_2O,O}+\rho_{H_2O}gh_{H_2O,O}$$

$V=Av$

$A=0.25\pi D^2$

Where $P_{H_2O,I}$ = Inlet pressure of water, kPa

$v_{H_2O,I}$= Inlet velocity of water, m/s

$h_{H_2O,I}$ = Inlet height of water from reference point, m

$P_{H_2O,O}$ = Outlet pressure of water, kPa

$v_{H_2O,O}$ = Outlet velocity of water, m/s

$h_{H_2O,O}$ = Outlet height of water from reference point, m

ρ_{H_2O} = Density of water, kg/m^3

g = Gravitational constant, m/s^2

V = Volumetric flowrate, ml/s

A = Tube area, mm^2

D = Tube diameter, mm

<u>Example determine outlet water flow rate of the system without water outlet pump</u>

Where $P_{H_2O,I}$= 91.325 kPa

$v_{H_2O,I}$= 0 m/s

$h_{H_2O,I}$ = 0 m

$P_{H_2O,O}$ = 103.62 kPa

$h_{H_2O,O}$ = 1.35 m

ρ_{H_2O} = 997 kg/m^3 at 25 °C

g = 9.81 m/s^2

D = 3.175 mm

$$P_{H_2O,I}+\frac{1}{2}\rho_{H_2O}v^2_{H_2O,I}+\rho_{H_2O}gh_{H_2O,I}=P_{H_2O,O}+\frac{1}{2}\rho_{H_2O}v^2_{H_2O,O}+\rho_{H_2O}gh_{H_2O,O}$$

$$91.325kPa+(\frac{1}{2}\times997\frac{kg}{m^3}\times0\frac{m}{s})+(997\frac{kg}{m^3}\times9.81\frac{m}{s^2}\times0m\times0.001\frac{kPa}{Pa}) =$$

$$103.62kPa+(\frac{1}{2}\times997\frac{kg}{m^3}\times v^2_{H_2O,O}\frac{m}{s})+(997\frac{kg}{m^3}\times9.81\frac{m}{s^2}\times1.35m\times0.001\frac{kPa}{Pa})$$

$v_{H_2O,O}$ = 0.04 $\frac{m}{s}$

A = 0.25πD^2

A = 0.25$\times$ π $\times$ 3.175^2

A = 7.917 mm^2

V = Av

V = 7.917mm^2$\times$0.04 $\frac{m}{s}$

V = 0.35 $\frac{ml}{s}$

Table B.2.1 Calculation of outlet flow rate of water from system without outlet pump and inlet flow rate of water to system.

System height 1.35 m & 1/3 psi CV			
Vaccuum (kPa)	**Height from tank to system (m)**	**Suction flowrate (ml/s)**	**Outlet flow rate (ml/s)**
0.50	0.50	-	1.15
1.00	0.50	-	1.12
1.50	0.50	-	1.09
2.00	0.50	-	1.06
2.50	0.50	-	1.03
3.00	0.50	-	1.00
3.50	0.50	-	0.97
4.00	0.50	-	0.93
4.50	0.50	-	0.90
5.00	0.50	3.45	0.86
5.50	0.50	8.64	0.83
6.00	0.50	11.72	0.79
6.50	0.50	14.14	0.75
7.00	0.50	16.21	0.70
7.50	0.50	18.04	0.66
8.00	0.50	19.70	0.61
8.50	0.50	21.23	0.55
9.00	0.50	22.66	0.49
9.50	0.50	24.00	0.43
10.00	0.50	25.27	0.35
10.50	0.50	26.48	0.24
11.00	0.50	27.64	-

Appendix B.3 Calculation of nozzle geometry

Calculation of throat section and diverging section areas of nozzle

$$\frac{T_{CO_2}}{T_{CO_2,0}} = \left(1+\frac{k-1}{2}Ma^2\right)^{-1}$$

$$\frac{P_{CO_2}}{P_{CO_2,0}} = \left(1+\frac{k-1}{2}Ma^2\right)^{-k/(k-1)}$$

$$\frac{A}{A^*} = \frac{1}{Ma}\left[\left(\frac{2}{k+1}\right)\left(1+\frac{k-1}{2}Ma^2\right)\right]^{0.5(k+1)/(k-1)}$$

$$v_{CO_2}=\sqrt{2C_{pCO_2}\left(T_{CO_2,0}-T_{CO_2}\right)}$$

$$A^*=\frac{\dot{m}_{CO_2}}{\rho_{CO_2}v_{CO_2}}$$

$$A = 0.25\pi D^2$$

Where Ma = Mach number

T_{CO_2} = local temperature of carbon dioxide, K

$T_{CO_2,0}$ = inlet temperature of carbon dioxide, K

P_{CO_2} = local pressure of carbon dioxide, bars

$P_{CO_2,0}$= inlet pressure of carbon dioxide, bars

A = cross-sectional area, m^2

A^* = cross-sectional area at throat, m^2

k = specific heat capacity ratio

π = Pi constant

$\dot{m}_{CO_2}$ = carbon dioxide mass flow rate, kg/s

ρ_{CO_2} = carbon dioxide density, kg/m^3

v_{CO_2} = throat velocity of carbon dioxide, m/s

D_d = diameter at diverging section

D_t = diameter at throat section

Example determine throat section area

Where k = 1.63

$T_{CO_2,0}$ = 273 K

Ma = 1

$P_{CO_2,0}$= 35 bars

$\dot{m}_{CO_2}$= 0.005 $\frac{kg}{s}$

$$\frac{T_{CO_2}}{T_{CO_2,0}} = \left(1+\frac{k-1}{2}Ma^2\right)^{-1}$$

$$\frac{T_{CO_2}}{273K} = \left(1+\frac{1.28-1}{2}\times1^2\right)^{-1}$$

T = 239.47 K

$$\frac{P_{CO_2}}{P_{CO_2,0}} = \left(1+\frac{k-1}{2}Ma^2\right)^{-\frac{k}{k-1}}$$

$$\frac{P_{CO_2}}{35} = \left(1+\frac{1.28-1}{2}\times1^2\right)^{-1.28/(1.28-1)}$$

P_{CO_2} = 19.23 bars

C_{p,CO_2} = 1.30 kJ/kg·K (From Table A.1 in Appendix A)

$$v_{CO_2} = \sqrt{2C_{p,CO_2}\left(T_{CO_2,0}\text{-}T_{CO_2}\right)}$$

$$v_{CO_2} = \sqrt{2\times1.30\frac{kJ}{kg\cdot K}\times(273\text{-}239.47)K\times1000\frac{m^2/s^2}{kJ/kg}}$$

$$v_{CO_2} = 295.\ 26\frac{m}{s}$$

$$A^* = \frac{\dot{m}_{CO_2}}{\rho_{CO_2}v_{CO_2}}$$

$\rho = 52.54\ \frac{kg}{m^3}$ (From Table A.1in Appendix A)

$$A^* = \frac{0.005\frac{kg}{s}}{52.54\ \frac{kg}{m^3}\times295.26\frac{m}{s}}$$

$$A = 3.22\times10^{-7}m^2$$

Example determine diverging section area

Where $k = 1.28$

$P_{CO_2} = 19.23$ bars

$P_v = 0.8$ bars

$A^* = 3.22\times10^{-7}m^2$

$$\frac{P_v}{P_{CO_2}} = \left(1+\frac{k-1}{2}Ma_e^{\,2}\right)^{-k/(k-1)}$$

$$\frac{0.8\text{ bars}}{19.23\text{ bars}} = \left(1+\frac{1.28-1}{2}\times Ma_e^{\,2}\right)^{-1.28/(1.28-1)}$$

$Ma_e = 2.68$

$$\frac{A}{A^*} = \frac{1}{Ma}\left[\left(\frac{2}{k+1}\right)\left(+\frac{k-1}{2}Ma^2\right)\right]^{\frac{0.5(k+1)}{(k-1)}}$$

$$\frac{A}{3.22\times10^{-7}m^2} = \frac{1}{2.68}\left[\left(\frac{2}{1.28+1}\right)\times\left(1+\frac{1.28-1}{2}\times2.68^2\right)\right]^{0.5\times(1.28+1)/(1.28-1)}$$

$A = 3.68\times10^{-4}m^2$

<u>Example determine diameter at each section</u>

$A = 0.25\pi D^2$

Diameter at throat section

$3.22\times10^{-7} = 0.25\pi D_t^2$

$D_t = 6.40\times10^{-4}$ m

Diameter at diverging section

$3.68\times10^{-4} = 0.25\pi D_d^2$

$D_d = 2.16\times10^{-2}$ m

Ratio between diverging and throat diameter

$$\frac{D_d}{D_t} = \frac{2.16\times10^{-2}}{6.40\times10^{-4}}$$

$$\frac{D_d}{D_t} = 33.75$$

Appendix B.4 Calculation of the difference in water temperature

Calculation of the difference in water temperature

$\dot{Q}_{H_2O,s}=\dot{m}_{H_2O}C_{p,H_2O}\Delta T_{H_2O}$

$\dot{Q}_{CO_2,l}=\dot{m}_{CO_2}L_{CO_2}$

Where $\dot{Q}_{H_2O,s}$ = Rate of sensible heat of water, kJ/s

$\dot{m}_{H_2O}$ = Mass flow rate of water, kg/s

C_{p,H_2O} = Specific heat capacity of water, kJ/kg·K

ΔT_{H_2O} = Temperature difference between outlet and inlet of water, K

$\dot{Q}_{CO_2,l}$ = rate of latent heat transfer of carbon dioxide, kJ/s

$\dot{m}_{CO_2}$ = mass flow rate of carbon dioxide, kg/s

L_{CO_2} = latent heat of carbon dioxide, kJ/kg

Example of calculation of effect of liquid carbon dioxide mass flow rate on temperature difference of water

Where $\dot{m}_{H_2O}$ = 0.008 kg/s

C_{p,H_2O} = 4.18 kJ/kg·K

$\dot{m}_{CO_2}$ = 0.003 kg/s

L_{CO_2} = 230 kJ/kg

$\dot{Q}_{CO_2,l}=\dot{Q}_{H_2O,s}$

$$0.003\frac{kg}{s}\times 230\frac{kJ}{kg}=0.008\frac{kg}{s}\times 4.18\frac{kJ}{kg\cdot K}\times\Delta T_{H_2O}$$

ΔT_{H_2O}=20.63 K

Appendix B.5 Vacuum pressure at 30 bars inlet pressure

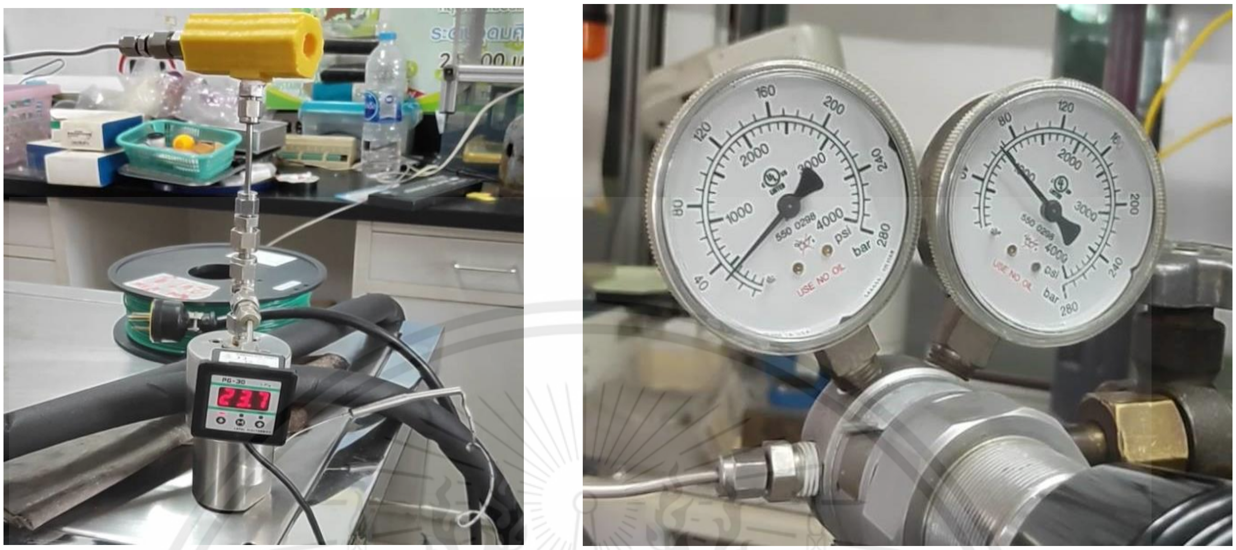

Figure B.5.1 Vacuum pressure at 30 bars inlet pressure.

Appendix B.6 Productivity of the system without pumping at downstream

Table B.6.1 Productivity of the system without pumping at downstream.

Tests	**Vacuum pressure (kPa)**	**Volumetric flow rate (ml/s)**
A	95.025	1.17
B	94.225	0.81
C	92.925	0.31

BIBLIOGRAPHY

Name: Taweechok Sochiphan

Date of Birth: March 18, 1999

Address: 43/10 Soi Nengaew 3, Nengaew Road, Thalahad Sub-district, Muang Dittrict, Suphanburi 72000

E-mail: taweechok36@gmail.com

Academic Background: Degree of Bachelor of Engineering
Department of chemical Engineering, School of Engineer
King Mongkut's Institute of Technology Ladkrabang